academicJournals

Vol. 9(9), pp. 303-310, 15 May, 2014
DOI: 10.5897/SRE2014.5907
Article Number: 8E4D96844494
ISSN 1992-2248 © 2014
Copyright©2014
Author(s) retain the copyright of this article
http://www.academicjournals.org/SRE

Scientific Research and Essays

Full Length Research Paper

Research on the transient radial force of the centrifugal pump

Wei Li[1,2*], Weidong Shi[1,2], Zhongyong Pan[1,2], Xiaoping Jiang[1,2] and Ling Zhou[1,2]

[1]Research Center of Fluid Machinery Engineering and Technology, Jiangsu University, Zhenjiang 212013, China.
[2]National Engineering Research Center of Pumps and Pumping System, Jiangsu University, Zhenjiang 212013, China.

Received 3 January, 2013; Accepted 2 March, 2013

The three-dimensional unsteady flow field in centrifugal pump under different flows was numerically simulated based on the commercial fluent software, using standard k-ε turbulence model, SIMPLE algorithm and sliding mesh technique. The characteristics of the time domain and frequency domain of the pressure pulsations, as well as fluctuation strength were analyzed. The varying locus of transient radial force vector of the centrifugal pump with time and the varying pattern of transient radial force with time were investigated. The results show that the frequencies of the pressure pulsations are mainly the blade passing frequency at the monitoring points, and the most intense pulsation appears at the volute tongue under the same frequency; the variation cycle of the transient radial force is the same with the passing cycle of the blades, and the direction of the radial force deflects anticlockwise as flow rate increases. At the designed flow rate, the distribution region of the radial force vector is the closest to the origin point and the area of the region is the smallest, with the gentlest fluctuation.

Key words: Centrifugal pump, transient radial force, pressure pulsation, numerical simulation.

INTRODUCTION

With the extensive application of large-scale centrifugal pumps in agricultural production, urban water supply and other fields, the requirements for the performance and stability of centrifugal pumps are increasing. The radial force greatly affects the efficiency and reliability of the pump, causing vibration and noise to the unit, and also fatigue failure to the shaft. Recently, with the development of the Computational Fluid Dynamics (CFD) and the computer technology, the unsteady numerical simulation is more and more widely applied in the studies of the characteristics of flow field (Meneveau and Katz, 2000; Kitano, 2005; Barrio et al., 2010; Spence and Amaral-Teixeira, 2009; González et al., 2002; Liu et al., 2013), and the numerical calculation of the unsteady force generated in centrifugal pumps has become an effective means (Ling et al., 2013). Kitano (2005) performed numerical simulation to the internal flow field of centrifugal pumps and pointed out that the unsteady characteristics of the internal flow vary in a periodic manner, and the flow causes intense pressure pulsation at the impeller outlet and inside the volute (Kelder et al., 2001; Longatte and Kueny, 2009; Wei et al., 2013). Jose et al. (2006) used unsteady numerical simulation to study the pattern that the transient radial force on the impeller

*Corresponding author. E-mail: lwjiangda@ujs.edu.cn
Author(s) agree that this article remain permanently open access under the terms of the Creative Commons Attribution License 4.0 International License

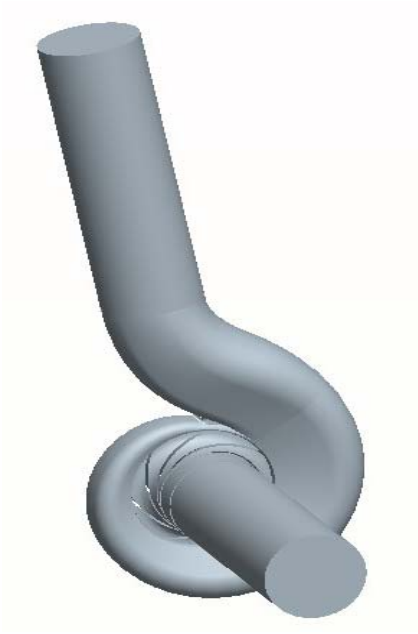

Figure 1. Model calculation domain.

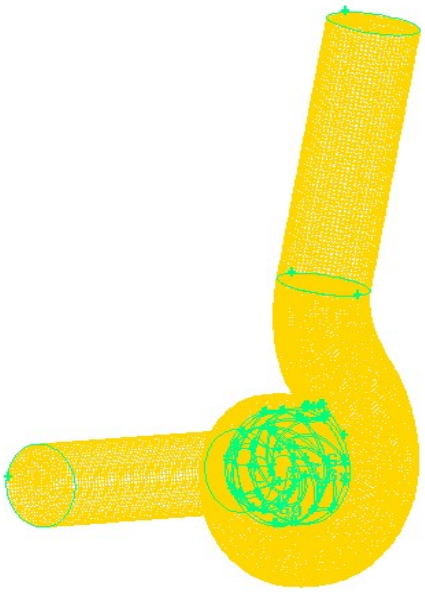

Figure 2. Mesh generation.

varies with time under different running conditions and volute tongue clearances (Adkins and Brennen, 1998; Brennen and Acosta, 2006; Guo and Okamoto, 2003). In this study, unsteady numerical calculation method is used to simulate the pressure pulsations of internal flow field in the centrifugal pump under three different running conditions; the characteristics of the time domain and frequency domain of the pressure pulsations, as well as their fluctuation strength are analyzed, and the locus of the variation of the centrifugal pump's transient radial force vector with time and the varying pattern of transient radial force with time are investigated.

The basic parameters of centrifugal pump are: designed rate of flow Q_d=1200 m^3/h, rated rotation speed

NUMERICAL CALCULATION MODEL AND METHODS

Simulation model

n=980 r/min, specific speed n_s=220, impeller outer diameter D_2=420 mm, outlet width b_2=85 mm, blade number z=7. Considering the complexity of the centrifugal pump structure, partitioning modeling is used for the convenience of mesh generation. The model calculation regions include the inlet pipe (1 m), the impeller, collector, and the outlet pipe (1 m), as shown in Figure 1. Gambit software is used for the mesh generation of the three-dimensional model, where for the impeller region and the collector region, unstructured tetrahedral mesh which is more adaptable to complex boundaries is adopted, and for the regions of the inlet pipe and the outlet pipe, structured hexahedral mesh is adopted; the total number of the meshes is about 500,000. The mesh generation of the pump model is shown in Figure 2.

Numerical calculation method

Based on fluent commercial software, the 3D incompressible N-S equation is used to describe the pump's interior flow, and the standard k-ε turbulence model close equations are adopted. The velocity inlet boundary condition is used for the inlet, the free outflow condition is used for the outlet, standard wall functions are used for regions close to the solid wall, and the non-slip boundary condition is for solid wall. Results from steady constant calculations are used for the initial flow field of the non-steady constant calculations, and $0.6Q_d$, Q_d and $1.4Q_d$ are selected as the three working conditions. The non-steady constant calculation uses the sliding mesh model to simulate dynamic and static interfere flow field, forming two mesh slip planes at the inlet and outlet of the impeller. The impeller meshes rotate relatively to those in other fluid regions, without the superposition of grid nodes on both sides of the interface. The calculations of all the fluid regions are executed at the same time. Discrete equations' solutions at each time step are worked out using SIMPLE algorithm. Time steps will be pushed forwards after calculation convergence, at the mean time, impeller meshes turn to a new position for new time step length calculation. The time step used in this paper is 1/360 of the impeller turning cycle (0.000170068 sec), that is, the time for the impeller to turn 1°. Iterative computation would stop after the data becomes relatively strict periodic on the monitor, and then the time-dependent curve of the centrifugal pump's transient radial forces is obtained.

NUMERICAL PREDICTION OF HYDRAULIC PERFORMANCE AND EXPERIMENTAL VERIFICATION

To verify the accuracy of the numerical simulation, the value of the experimental and numerical simulation of hydraulic performance in centrifugal pump were compared. The external characteristic curve is shown in Figure 3. The analysis on diagram shows that the external characteristics curve calculated by the numerical calculation agrees well with test results. The relative error

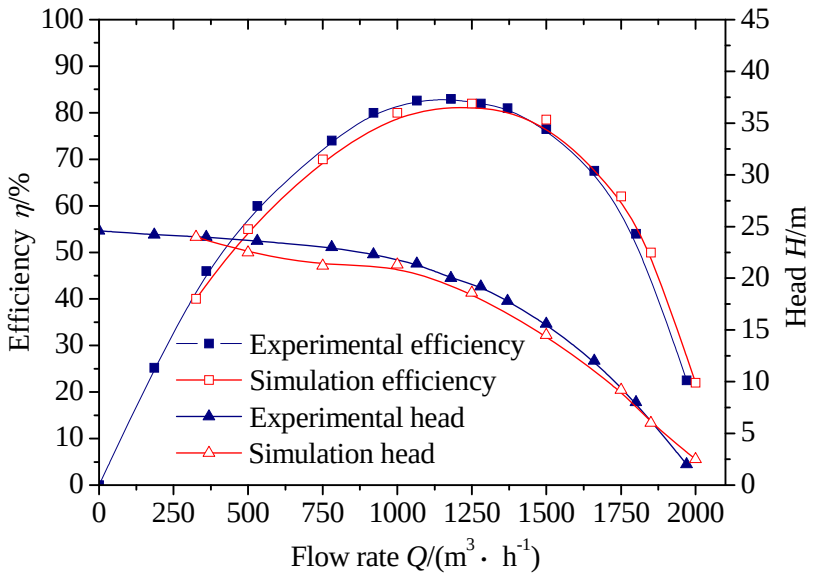

Figure 3. Comparison of external characteristics predicted curve and test curve.

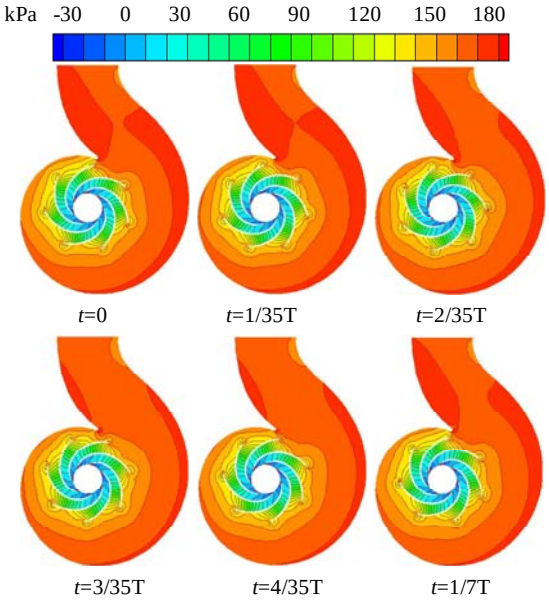

Figure 4. Static pressure distribution.

of the head and the efficiency were 2.6 and 2.0%, respectively, at maximum efficiency points of numerical calculation results and test results. The head and efficiency curves predicted by unsteady numerical calculation tend to below the test value. The main reason may be due to ignoring influence of the pump chamber and wall roughness on the performance of the pump. According to the analysis of test results and unsteady numerical calculation results, using the grid type, the turbulence model, etc. can more accurately predict the external characteristics of centrifugal pump.

STATIC PRESSURE DISTRIBUTION

The internal pressure distribution of the centrifugal pump changes with the impeller rotation. Let T be the time cost by one rotation of the impeller, since the impeller of the model has 7 blades, the passing cycle for each blade is 1/7T. Figure 4 presents the static pressure distribution of the impeller and volute areas under designed flow rate at the different time points in one blade passing cycle (1/7T).

It can be seen that in one blade passing cycle, the pressure of the area around the volute tongue varies significantly. When the blade passes by the volute tongue, the pressure of the area around the volute tongue reaches the lowest point; and when the blade goes away from the volute tongue, the pressure of the area increases gradually. At the inlet of the volute, an apparent low pressure area appears in the area that the tip of the blade passes by. Because of the dynamic-static interference between the impeller and the volute, as the relative location of the blade with the volute tongue changes, the static pressure distribution inside the volute shows a periodic change. The discrepancy of the internal pressure distributions inside the flow channel at different times is exactly the result of the dynamic-static interference between the impeller and the volute.

ANALYSIS OF PRESSURE PULSATION

Eight pressure monitoring points are set along the spiral direction of the centrifugal pump volute at the near-wall

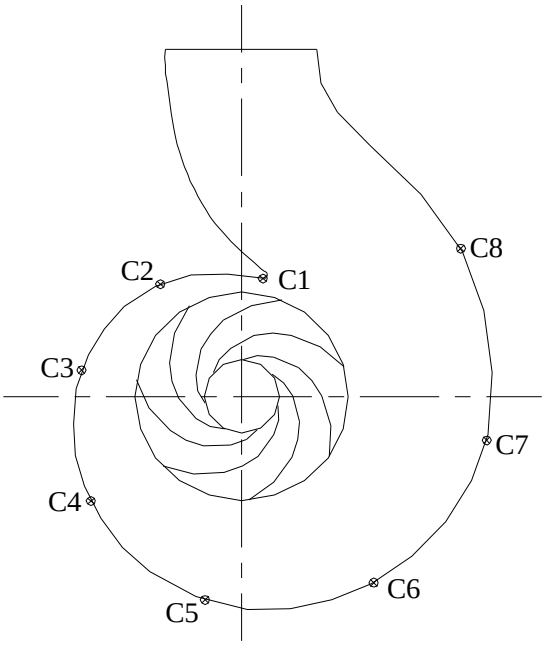

Figure 5. Pressure monitoring points.

side of eight sections of the volute. The monitoring points are named as C1~C8, while C1 is located at the volute tongue. The distribution of the monitoring points is as shown in Figure 5.

Analysis on the time domain of the pressure pulsation

Figure 6 presents the time domain charts of the pressure variations at different monitoring points of the model pump under the three running conditions of $0.6Q_d$, Q_d and $1.4Q_d$. The T in the figures indicates the time it takes for one rotation of the impeller. It can be seen from the charts that the pressure fluctuations of each point have basically consistent forms; they all have seven peaks and seven troughs, but with different amplitudes. The pressures gradually decrease with the increase of the flow rate, the amplitudes of the pulsations increase as the flow rate increases, and the difference of the pressure pulsation amplitudes in different region gradually decreases with the increase of the flow rate. Under the running condition with low flow rate, the amplitudes of the pressure pulsations from the volute tongue to Section III decrease significantly, and at Section III the flow basically stabilizes, as shown in Figure 6(a). Under the designed running condition, except for the C1 point at the volute tongue, the pressures of the other monitoring points are close, with slight increase along the spiral direction of the volute; in particular, for C5-C8, since they are far away from the volute tongue, the pressure pulsations are almost identical for these points; at the volute tongue, due to the

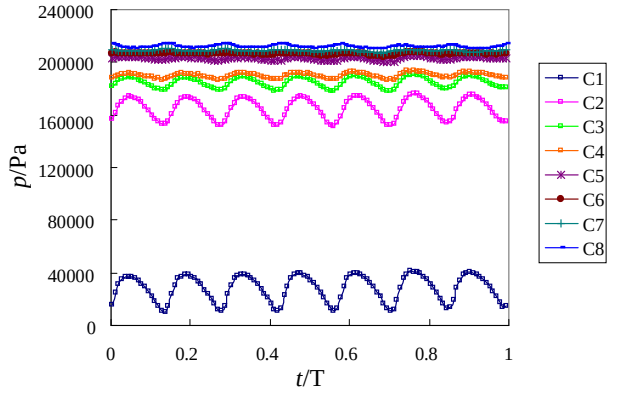

(a) Q=0.6Q_d

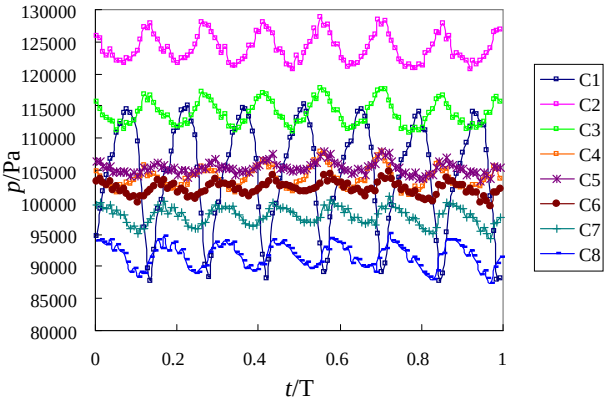

(b) Q=Q_d

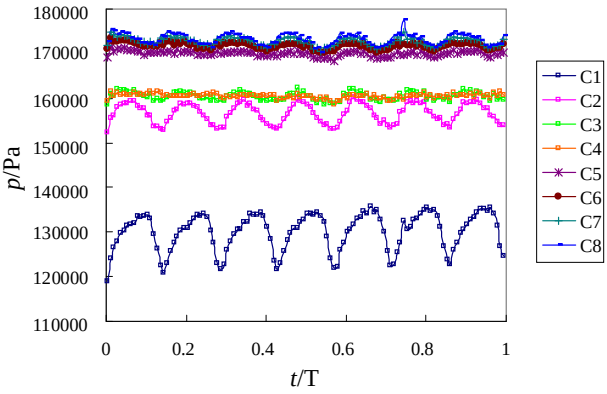

(c) Q=1.4Q_d

Figure 6. Pressure pulsation time domain charts.

complex fluid condition and the large pressure change gradient, the pressure of this point is quite different with other monitoring points, however, the pulsations are in pattern, the pressure change is shown in Figure 6(b). Under the running condition with large flow rate, the

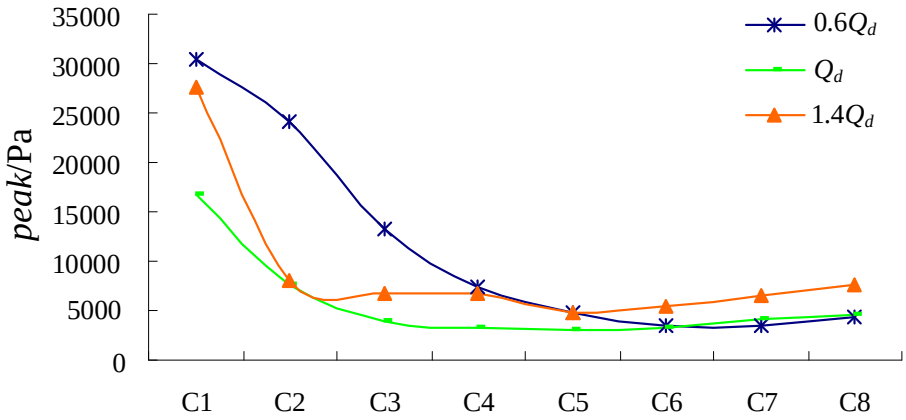

Figure 7. Peak curve of the pressure pulsation.

pressure pulsation amplitudes of the monitoring points are all large, with more disordered flow; the pulsation amplitude of the C1 point at the volute tongue is more than three times of the amplitudes of other points; the pressure of C2-C8 gradually decrease along the spiral direction of the volute, as shown in Figure 6(c).

Contrast on the peaks of the pressure pulsations

The pressure pulsation peak situation at each monitoring points along the spiral direction of the volute is shown in Figure 7. As can be seen from Figure 7, the maximum peak of the pressure pulsation is located in volute tongue position, the peaks of the pressure pulsations from the volute tongue to Section III sharp decline, and the peaks of the pressure pulsations from Section III to the volute outlet direction change more gentle, which accord with the analyzing results of the pressure pulsation time domain. Contrast can be seen, the peaks of pressure pulsations at each monitoring points under the non-design conditions always have a higher level, significantly greater than the designed running condition, and towards the outlet of the volute, the peaks pressure pulsations under the running condition with large flow rate are maximum, the peaks of the pressure pulsations under the design conditions and the running condition with low flow rate are basically consistent.

Analysis on the frequency domain of the pressure pulsation

The rotation speed of the impeller is 980 r/min, then the rotation frequency of the principle shaft is 16.333 Hz. For the number of blades is z=7, the blade passing frequency is 114.333 Hz. Convert the pressure pulsation data of the monitoring points through Fast Fourier Transform (FFT), and then the pressure pulsation frequency domain charts of the monitoring points could be obtained. Investigation shows that at each monitoring point, the frequency of the pressure pulsation is mainly blade passing frequency, followed by the doubled blade frequency, and under the same frequency the most intense pulsation appears at the volute tongue. The intensity of the pressure pulsations at each monitoring points under the blade passing frequency is shown in Figure 8, where the vertical coordinate is index coordinate. It can be seen that the pressure pulsation of the C1 point at the volute tongue is the most intense under different flow rates. With the increase of the flow rate, the intensity of the pressure pulsations of all the monitoring points increase, which accord with the analyzing result of the pressure pulsation time domain.

ANALYSIS OF THE TRANSIENT RADIAL FORCE

Variation of the transient radial join force in one rotation cycle of the impeller

Due to the coupling effect between the blades and the collector, the strength and direction of the radial force on the impeller always change in an approximate periodic manner within a certain range as the impeller rotates, where the cycle is related to the number of the blades. At the flow rates of 0.6Q_d, Q_d, and 1.4Q_d, the vector locus of the transient radial force on the model impeller in one rotation cycle T is shown in Figure 9.

It could be seen from Figure 9 that the vector locus of the pump model's transient radial forces under the three different flow rates are significantly different. When the flow rate is 0.6 Q_d or Q_d, the locus of the transient radial force are in the second quadrant, and the distributed regions have respectively 40° and 75° angles with the y axis; and when the flow rate is 1.4Q_d, the trail is in the fourth quadrant, with a 135° angle with the y axis. Meanwhile, at the flow rate of 0.6Q_d, the distributed

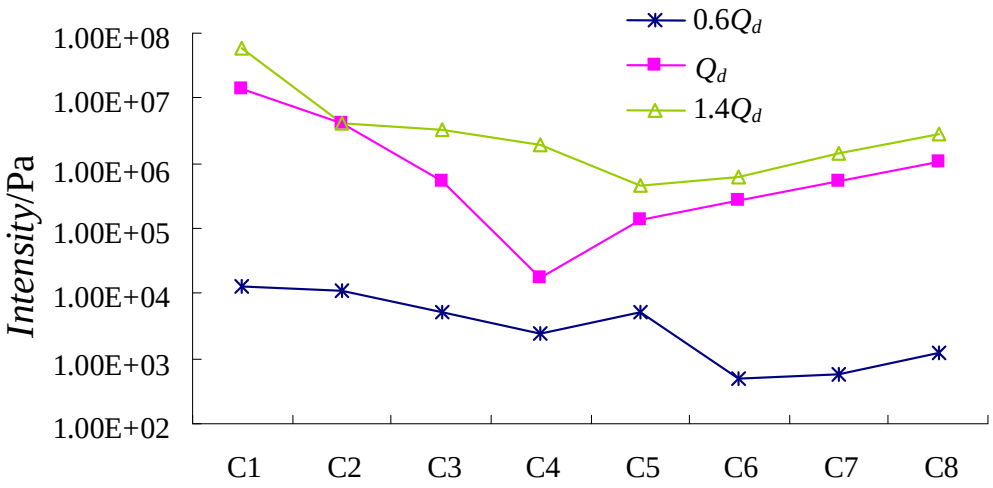

Figure 8. Intensity comparison of the pressure pulsations.

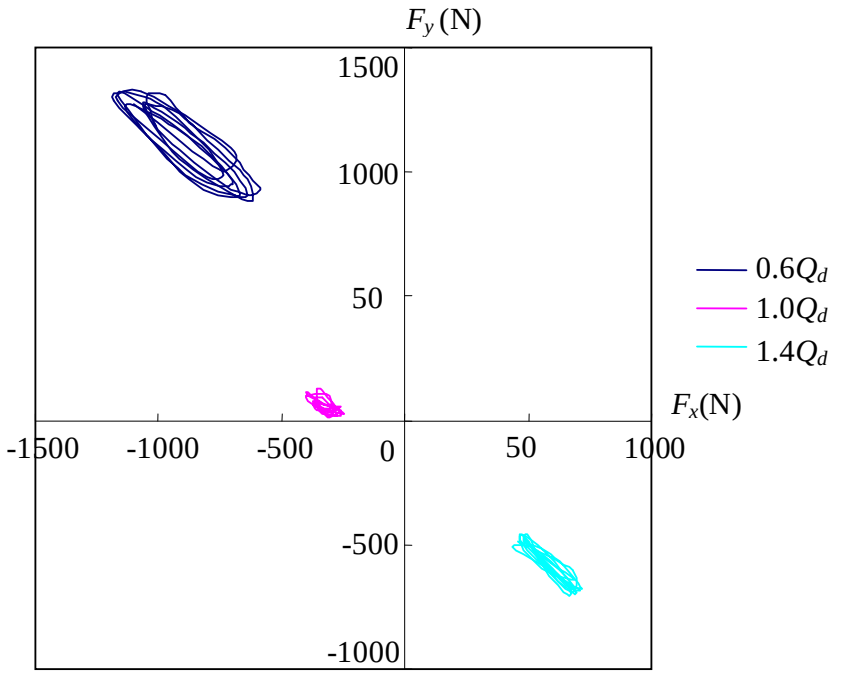

Figure 9. Vector locus of the transient radial force.

region of the transient radial force locus is the farthest from the origin of the coordinate system, and the area of the region is the largest; at the designed flow rate, the distributed region of the transient radial force locus is the closest to the origin, with the smallest area. It is indicated that the radial force on the impeller is the smallest under the designed running condition. From the distributed locations of the vector locus of the transient radial forces under different flow rates, it can be seen that the direction of the radial force on the impeller changes anticlockwise with the increase of the flow rates.

Variation of the transient radial join force in one rotation cycle of the impeller

The time domain charts of the variation of the transient radial join force during one rotation cycle T of the impeller under the three running conditions of 0.6Q_d, Q_d and 1.4Q_d is shown in Figure 10. It can be seen from Figure 10 that

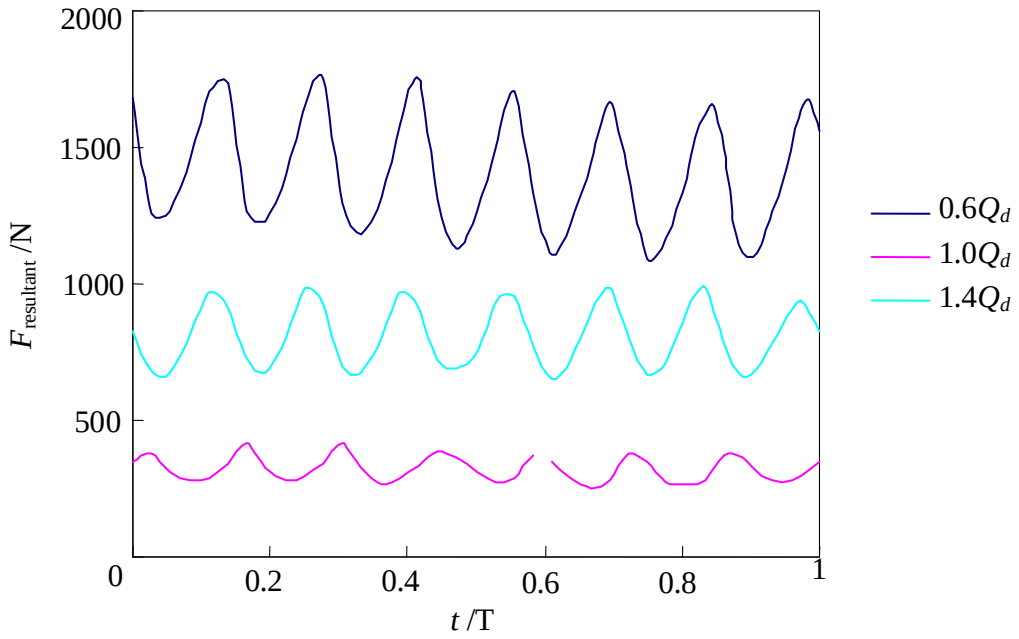

Figure 10. Time domain diagram of the transient radial force on the impeller.

the transient radial forces on the impeller under different flow rates show periodic fluctuations, with seven major peaks and troughs, where the number is the same with the number of the impeller blades and the fluctuation of each cycle is similar, indicating that the transient radial force on the impeller changes periodically with the rotation of the blades. The order of the three running conditions with small to large transient radial join forces is Q_d, $1.4Q_d$, $0.6Q_d$, so is the order of the three running conditions with small to large amplitudes of the periodic fluctuations of the transient radial join force. Thus, the running condition with small flow rate is the most unstable with the largest transient radial force, and the designed running condition is the most stable with the smallest transient radial force.

Conclusions

The pressure in the centrifugal pump shows periodic pulsations as the impeller rotates, where the amplitude of the pressure pulsation is the largest at the volute tongue. The main frequency of the pressure pulsations is the blade passing frequency, which is 114.333 Hz, indicating that the dynamic-static interference between the blades of the impeller and the collector is the major factor causing the pressure pulsation.

The radial force on the impeller of the centrifugal pump varies periodically during the rotation of the impeller, with the blade passing cycle as its varying cycle. Under non-designed flow rates, the radial force on the impeller is large, and the amplitude of the fluctuation is the largest under the running condition with small flow rate; under designed flow rate, the transient radial force on the impeller is small, with gentle fluctuations.

Conflict of Interests

The author(s) have not declared any conflict of interests.

ACKNOWLEDGMENTS

This work was sponsored by the Natural Science Foundation Project of Jiangsu Province (No.BK2011505), PAPD, National Science and Technology Support Program of China (No. 2011BAF14B01), Agricultural Science and Technology Support Program of Zhenjiang City (No. NY2013031), Postdoctoral Science Foundation of China (No.2013M541614), Postdoctoral Science Foundation of Jiangsu Province (No.1301062C).

REFERENCES

Adkins DR, Brennen CE (1998). Analysis of hydrodynamic radial forces on centrifugal pump impellers. J. Fluids Eng. 110(3):20-28.

Barrio R, Parrondo J, Blanco E (2010). Numerical analysis of the unsteady flow in the near-tongue region in a volute-type centrifugal pump for different operating points. Comput. Fluids (39):859-870. http://dx.doi.org/10.1016/j.compfluid.2010.01.001

Brennen CE, Acosta AJ (2006). Fluid-induced rotordynamic forces and instabilities. Struct. Control Health Monit. 13(1):10-26. http://dx.doi.org/10.1002/stc.145

Guo S, Okamoto H (2003). An experimental study on the fluid force induced by rotor-stator interaction in a centrifugal pump". Int. J.

Rotating Machinery 9(2):135-144. http://dx.doi.org/10.1155/S1023621X03000125

Jose G, Jorge P, Carlos S, Eduardo B (2006). Steady and unsteady radial forces for a centrifugal pump with impeller to tongue gap variation. J. Fluids Eng. (128):454-462.

Kelder JDH, Dijkers RJH, Van Esch BPM (2001). Experimental and theoretical study of the flow in the volute of a low specific-speed pump. Fluid Dynamics Res. (28):267-280. http://dx.doi.org/10.1016/S0169-5983(00)00032-0

Kitano Majidi (2005). Numerical study of unsteady flow in a centrifugal pump. J. Turbomachinery.127(2):363-371. http://dx.doi.org/10.1115/1.1776587

Ling Zhou, Weidong Shi, Wei Li (2013). Ramesh Agarwal. Numerical and experimental study of axial force and hydraulic performance in a deep-well centrifugal pump with different impeller rear shroud radius. J. Fluids Eng. 135:104501-8. http://dx.doi.org/10.1115/1.4024894

Liu H, Wang K, Kim H, Tan M (2013). Experimental investigation of the unsteady flow in a double-blade centrifugal pump impeller. China Technol. Sci. 56(4):812-817. http://dx.doi.org/10.1007/s11431-013-5154-0

Longatte F, Kueny JL (2009). Analysis of rotor-stator-circuit interactions in a centrifugal pump. Proceedings of the 3rd ASME/JSME Joint Fluids Engineering Conference. pp.1039-1045.

Meneveau C, Katz J (2000). Scale-invariance and turbulence models for large-eddy-simulation. Annu. Rev. Fluid Mech. (32):1-32. http://dx.doi.org/10.1146/annurev.fluid.32.1.1

Spence R, Amaral-Teixeira J (2009). A CFD parametric study of geometrical variations on the pressure pulsations and performance characteristics of a centrifugal pump. Comput. Fluids. (38):1243-1257. http://dx.doi.org/10.1016/j.compfluid.2008.11.013

Wei L, Weidong S, Yandong X, Ling Z, Pingping Z (2013). Effects of guide vane thickness on pressure pulsation of mixed-flow pump in pumped-storage power station. J. Vibroeng15(3):1077-1085.